COBEM 99
XV Congresso Brasileiro de Engenharia Mecânica
15th Brazilian Congress of Mechanical Engineering
22 - 26 de Novembro de 1999 / November 22 - 26, 1999 Águas de Lindóia, São Paulo,

BULK CHARACTERISTICS OF SOME VARIABLE VISCOSITY POLYMER SOLUTIONS IN TURBULENT PIPE FLOW

A. S. Pereira
Departamento de Engenharia Química, Instituto Superior de Engenharia do Porto
Rua de São Tomé, 4200 Porto, Portugal
F. T. Pinho
Centro de Estudos de Fenómenos de Transporte, DEMEGI, Faculdade de Engenharia,
Universidade do Porto, Rua dos Bragas, 4099 Porto Codex, Portugal, fpinho@fe.up.pt

Abstract. *As part of a research programme on wall-free turbulent flows of non-Newtonian fluids, aqueous solutions of three different polymers have been extensively investigated in terms of their frictional pressure drop versus flow rate characteristics, after a carefull process of fluid selection and rheological characterisation reported elsewhere (Pereira and Pinho, 1994 and Coelho and Pinho, 1998). All solutions, and in particular those of CMC and more so of xanthan gum, exhibited drag reduction. The total drag reduction was separated into shear-thinning (* DR_V *) and elastic (* DR_e *) contributions, with* DR_V *reaching a maximum of about 30% of the total for the thickest xanthan gum solutions.*

Keywords: *Drag reduction; Pipe flow*

1. INTRODUCTION

The inadequacy of conventional rheological tests and theory to allow extrapolation from measured rheological properties to the hydrodynamic characteristics of non-Newtonian viscoelastic fluids in turbulent flows is a known limitation. To compensate for this shortcoming it has been recomended by Pereira and Pinho (1994) that, prior to the investigation of complex turbulent flows of non-Newtonian fluids, these fluids should be investigated in terms of pressure drop versus flow rate characteristics in circular pipe. In particular, the pipe flow data provides information on the extension of the drag reduction phenomenon which has long been associated by many authors to be an elastic response of the fluids (Lumley 1977). This should help the interpretation of results of investigations on more complex turbulent flows.

According to some theories the reduction of the friction coefficient in turbulent pipe flow of very dilute polymer solutions is due to elongational effects. Hinch (1977), O'Shaughnessy et al (1990) and more recently Kostic (1994) amongst many others, argue that this could be related to a strong strain-imposed resistance to elongation of the molecules and its effects upon the extensional viscosity of the fluids. Thus, the magnitude of the viscosity would be larger than in the absence of such elongational deformations. Periodically, the increased elongational viscosity argument is combined (or substituted) with arguments based on viscosity anisotropy (see Hoyt 1972 and Myska 1998).

These tentative theories have recently gained strength from the works of Den Toonder et al (1995) and Orlandi (1995), who carried out direct numerical simulations with non-Newtonian fluids having a strain-thickening viscosity and were able to predict some drag-reduction and the correct trends in the Reynolds stresses. The availability of DNS techniques is currently giving a new impetus to those theoretical arguments and allowing testing of rheological models exhibiting different viscoelastic behaviour, as can be assessed from Massah and Hanratty (1996) and Massah et al (1993).

The hydraulic behaviour of viscoelastic non-Newtonian fluids in turbulent pipe flow is quite different from that of Newtonian or purely viscous non-Newtonian fluids. Their friction factor is substantially lower and this drag reduction usually increases with the flow rate, the polymer molecular weight and the polymer concentration and is also affected by the flexibility of the molecules. In addition, the diameter of the pipe, the degree of degradation of the polymer and the chemistry of the solvent are important parameters in the determination of the drag-reduction intensity. The extent of the drag-reduction is ultimately limited by a unique envelope asymptote derived in the late sixties and well documented in the reviews of Hoyt (1972) and Virk (1975). This asymptote is independent of the polymer, polymer concentration, solvent chemistry, or the degree of polymer degradation and is dependent solely on the Reynolds number, Hartnett (1992), but is only adequate for some polymer solutions and other classes of non-Newtonian fluids, such as surfactants, may tend to other asymptotes (Zakin et al 1996).

The research must be extended to other classes of turbulent flows as wall-free turbulent flows of non-Newtonian fluids. As part of one such programme aqueous solutions of three different polymers have been extensively investigated in terms of their pressure drop- flow rate behaviour in pipe flow, after a careful process of fluid selection and rheological characterisation reported elsewhere (Pereira and Pinho 1994, Coelho and Pinho 1998), and it is the result of this extensive bulk flow characterisation that is reported in this paper.

The remaining of the paper is organised as follows: the fluids and their rheology are presented first and is followed by a description of the flow rig. Then, the pressure drop- flow rate measurements are presented and discussed.

2. FLUIDS

The fluids under investigation are aqueous solutions of three different polymers, tylose, grade MH 10000K from Hoechst, carboxymethil cellulose (CMC), grade 7H4C from Hercules, and xanthan gum (XG), grade keltrol TF from Kelco, at weight concentrations of 0.1% to 0.6%, 0.1% to 0.4% and 0.05% to 0.25%, respectively. These fluids were chosen for reasons explained elsewhere (Pereira and Pinho 1994, Pinho and Whitelaw 1990 and Escudier et al 1995) after a careful process of fluid selection but here we summarise their main rheological characteristcs. To all solutions 0.02% by weight of kathon LXE from Rohm and Haas was added to prevent against bacteriological degradation.

2.1 Tylose solutions

The low molecular weight of this additive (6000 kg/kmole) produces weakly shear-thinning solutions of very low elasticity and the viscometric viscosity is well fitted by a Carreau-Yasuda model (Eq. 1)

$$\eta = \eta_\infty + \left(\eta_0 - \eta_\infty\right)\left[1+\left(\lambda\dot{\gamma}\right)^a\right]^{\frac{n-1}{a}} \tag{1}$$

with the corresponding parameters given in Table 1.

According to Coelho and Pinho (1998), the thickest solution (0.6% tylose) did not exhibit significant elasticity in the creep test, and in oscillatory shear flow the ratio of the loss to storage moduli G"/G' varied between 3.2 and 4 for frequencies ranging from 5 to 16 Hz and increasing for higher frequencies.

Table 1- Parameters of the Carreau-Yasuda model for the solutions of tylose and CMC at 25°C. Data from Coelho and Pinho (1998) and Coelho et al (1996)

Solution	η_o[Pas]	η_∞[Pas]	λ[s]	a	n	$\dot{\gamma}$[s^{-1}]
0.1% Tyl.	0.00228	0.001	0.0000975	0.350	0.7275	100 to 3000
0.2% Tyl.	0.00608	0.001	0.00012	0.3008	0.6111	20 to 4000
0.3% Tyl.	0.0107	0.001	0.00090	0.6592	0.5856	10 to 4000
0.4% Tyl.	0.02276	0.001	0.00300	0.7432	0.6051	10 to 4000
0.5% Tyl.	0.04190	0.001	0.00255	0.6777	0.49448	2 to 4000
0.6% Tyl.	0.06924	0.00148	0.00751	1.1172	0.5572	5 to 4000
0.1% CMC	0.01319	0.0005	0.01922	0.8086	0.6464	10 to 4000
0.2% CMC	0.03454	0.000928	0.02771	1.216	0.5875	30 to 4000
0.3% CMC	0.1005	0.000813	0.04575	0.6504	0.5094	1 to 4000
0.4% CMC	0.1575	0.000898	0.06784	1.016	0.5137	1 to 4000

2.2 CMC solutions

CMC has a longer, flexible molecule than tylose (3×10^5 kg/kmole) thus imparting a mildly shear-thinning behaviour to the aqueous solutions and more elasticity. The viscosity is again well fitted by the Carreau-Yasuda model and the corresponding parameters are also included in Table 1.

The CMC solutions have low elasticity, but higher than that of the tylose solutions, as measured in both the creep test and the oscillatory shear test. The relaxation times measured in the creep test for some of solutions are compared in Table 2. Clearly, the CMC solutions are more elastic than the tylose at identical additive concentration, but less than the xanthan gum solutions.

The ratio G"/G' now varies from 1.5 at 5 Hz to 1.3 at 20 Hz and then increases to about 1.7 at 35 Hz.

Table 2- Relaxation times of some solutions measured in creep (from Coelho and Pinho, 1998 and Coelho et al, 1996)

	0.4% CMC	0.3% CMC	0.2% CMC	0.1% CMC	0.6% Tyl.	0.4% Tyl.
λ_e[s]	0.463	0.332	0.097	0.046	0.389	0.06
	0.125% XG	0.15% XG	0.2% XG	0.25% XG		
λ_e[s]	1.089	2.435	4.27	8.66		

2.3 Xanthan gum solutions

The molecules of xanthan gum are the longest and heaviest (2×10^6 kg/kmole) and the fluid exhibits a strong shear-thinning behaviour where the low shear rate Newtonian plateau could not be detected in the measured range of shear rates, but the tendency for stabilisation at high shear rates is observed. For this reason the viscosity of the xanthan gum solutions is better fitted by the Sisko model (Eq. 2)

$$\eta = \eta_{ref}\left(\lambda_s\dot{\gamma}\right)^{n-1} + \eta_\infty \qquad (2)$$

whose parameters are presented in Table 3.

Finally, to better understand the relative viscosity behaviour of the various solutions, the corresponding fitted models are directly compared in Fig. 1.

Table 3- Parameters of the Sisko model for the solutions of xanthan gum at 25°C

Solution	$\eta_{ref}[Pas]$	$\eta_{\infty}[Pas]$	$\lambda_s[s]$	n	$\dot{\gamma}[s^{-1}]$
0.05% XG	0.016743	0.000334	2.5	0.6986	10-1600
0.1%XG	10.52	0.0012	1970	0.4299	2-3300
0.125%XG	15.94	0.00131	1999	0.4028	1-3000
0.15%XG	21.99	0.00133	1980	0.3859	0.6-3500
0.2%XG	58.06	0.001589	1900	0.3434	0.06-4100
0.25%XG	98.54	0.001769	1700	0.3256	0.07-4100

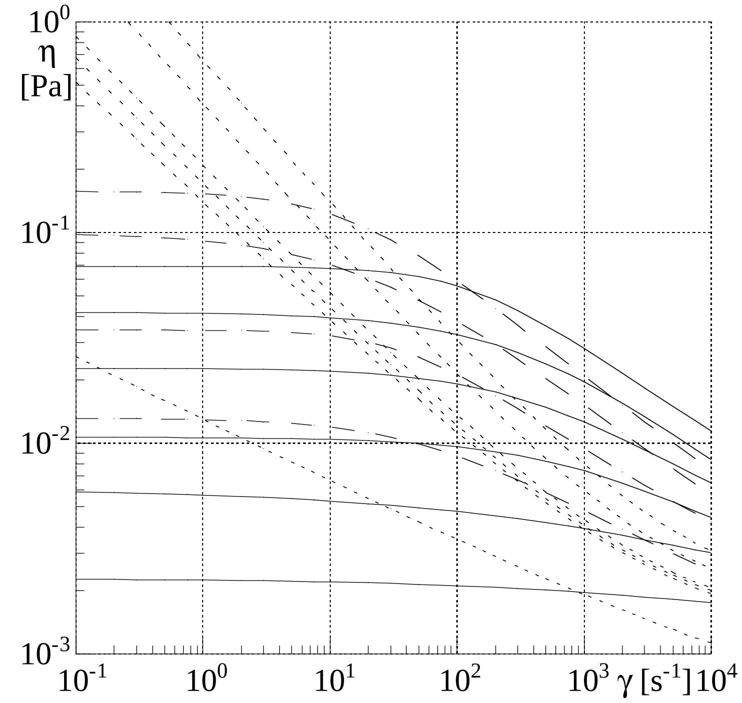

Figure 1- Comparison between the viscometric viscosity of all solutions in Tables 1 and 3. Data plotted are the fitted viscosity models. (Solid line: tylose solutions; long dashes: CMC solutions; short dashes: xantham gum. Higher concentrations have higher viscosities).

3. EXPERIMENTAL FACILITY

The flow configuration used in the present experiments has been previously described in Pereira and Pinho (1994), and consisted of a long 26 mm inside diameter vertical pipe. The fluid circulated in a closed vertical circuit, pumped from a 100 liter tank along a rising pipe and then through a 90 diameter long descending pipe to the transparent acrylic test section of 232 mm length, and a further 27 diameters down to the tank. The flow was controlled by means of two valves and a by-pass circuit. The transparent test section was used in LDA measurements not reported here. A 100 mm long honeycomb was located 90 diameters upstream of the test section to help ensure a fully-developed flow in the plane of the measurements. Four pressure taps were drilled in the test section and in the upstream pipe and were used for the pressure measurements. Equal longitudinal pressure gradients were measured between consecutive pairs of taps which, together with equal velocity profile measurements at two different stations within the test section, confirmed a fully developed flow situation.

An electromagnetic flowmeter from ABB Kent-Taylor, model Mag Master, was incorporated in the rising pipe of the flow loop. The output of the flowmeter was sent to a 386 PC by a data acquisition Metrabyte DAS-8 board interfaced with a Metrabyte ISO 4 multiplexer, both manufactured by Keithley. The flowmeter was capable of measuring the volumetric flow rate in the range 0-5 l/s with a stated accuracy of 0.04% of full scale. To check the accuracy of the flow meter, LDA measurements of the mean velocity profile were carried out with water and the corresponding integrated bulk velocity differed by less than 1% from that given by the flowmeter, therefore we will consider here a total bulk velocity uncertainty of 1% of the reading.

The pressure variation was simultaneously measured by means of two differential pressure transducers, models P305D-S20 and P305D-S24 from Validyne, and their output was sent to the same computer through the same data acquisition board. The uncertainty of the friction factor values was estimated to range from ± 7.5% at the lowest values of the Δp (lowest Reynolds numbers in laminar flow) to ± 2.5% at the maximum Reynolds numbers.

4. RESULTS AND DISCUSSION

Several issues will be discussed in this paper namely, the effect of polymer additive type and concentration on the fRe behaviour, with emphasis on the drag reduction, and the amounts of drag reduction due to elasticity and purely viscous (shear-thinning) effects.

Studies of drag reduction for very dilute solutions of constant viscometric viscosity abound in the literature, but there are only a few related to variable viscosity fluids (Pinho and Whitelaw 1990, Pinho and Pereira 1994, Escudier et al 1992, 1999, amongst others). In any case, there is consensus that the relevant viscosity to be used for normalisation, say in the Reynolds number of Eq. 3, is the viscosity at the shear rate prevailing at the wall. U stands for bulk velocity of the fluid of density ρ and D is the pipe diameter. The wall viscosity corresponds to the wall shear stress determined from the pressure drop measurements and the measured viscosity behaviour.

$$\mathrm{Re}_w \equiv \frac{\rho U D}{\eta_w} \tag{3}$$

For variable viscosity fluids the drag reduction $\left(DR \equiv \left(f - f_N\right)/f_N\right)$ is defined in relation to the Newtonian friction factor at the same wall Reynolds number (f_N). However, a second quantity is required as purely viscous shear-thinning fluids do have some degree of drag reduction, ie, the total drag reduction for a viscoelastic shear-thinning fluid is actually the sum of a purely viscous effect and an elastic effect. The viscous drag reduction (DR_v) is the relative difference between the friction factor of a purely viscous shear-thinning fluid, which was derived by Dodge and Metzner (1959), and that of a Newtonian fluid at the same wall Reynolds number. To calculate DR_v, it is advantageous to cast Dodge and Metzner's equation in terms of the Darcy friction factor, the definition used in this work, and to transform their generalized Reynolds number into a wall Reynolds number leading to

$$\frac{1}{\sqrt{f}} = 0.8685 n^{0.25} \ln\left(\frac{2n}{3n+1}\mathrm{Re}_w \sqrt{f}\right) + \frac{2.4095}{n^{0.75}}(1-n) - \frac{0.2}{n^{1.2}} \tag{4}$$

Eq. (4) requires the power index n of a power law viscosity model and is plotted in Fig. 2 for several decreasing values of n. The figure shows clearly the aforementioned drag reduction due to shear-thinning intensity. The effect is stronger at low Reynolds numbers and higher degrees of shear-thinning and can even lead to a value of f lower than that predicted by Virk's asymptote (cf. Fig. 2). As the intensity of shear-thinning increases, fluids are likely to be thicker and will not attain high Reynolds number flows, so the DR_v effect will be significant.

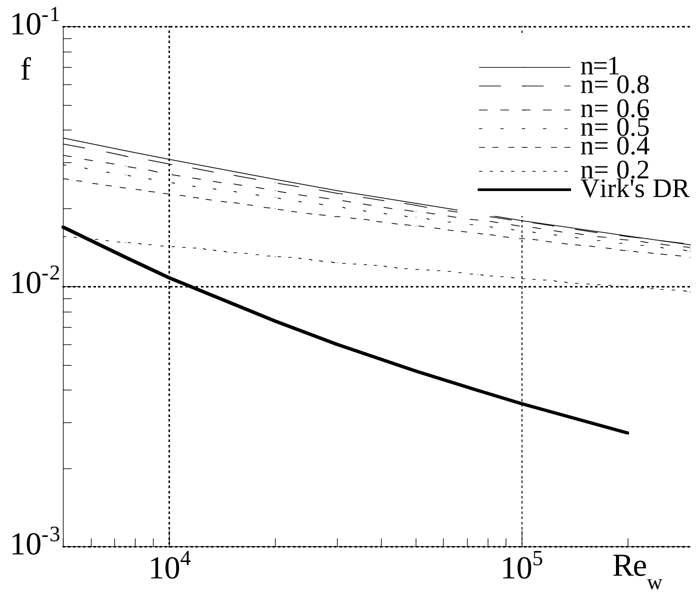

Figure 2- Variation of the friction factor for purely viscous shear-thinning fluids as a function of the wall Reynolds number, according to Dodge and Meztner (1959)

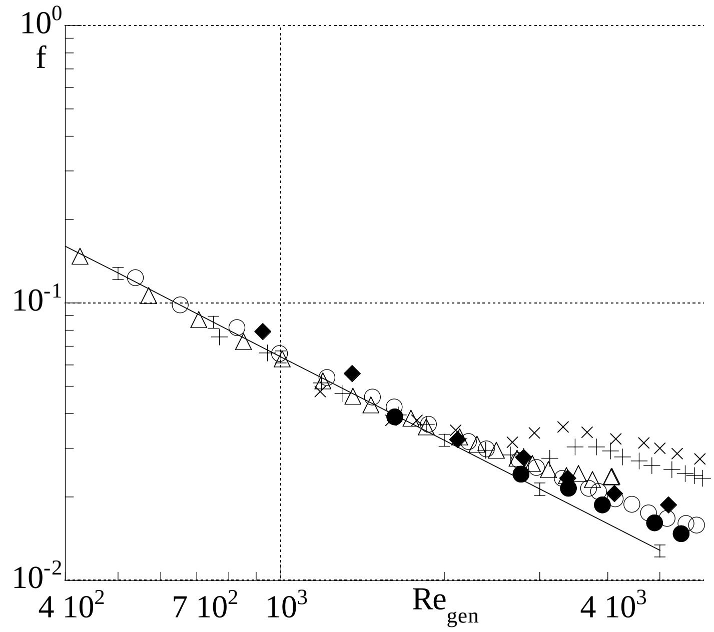

Figure 3) Darcy friction factor versus generalized Reynolds number in the laminar regime. x 0.4% tylose; + 0.5% tylose; Δ 0.6% tylose; O 0.4% CMC; J 0.2% XG; F 0.25% XG. Bars on the straight line correspond to ±5%

Measurements of the Darcy friction factor *f* were carried out for all fluids mentioned in Section 2 and water, at the laminar and turbulent regimes. The quality of the measurements can be assessed in Fig. 3 which compares some measured values of *f* with the theoretical expression derived by Metzner and Reed (1955) for laminar flow

$$f = 64/\mathrm{Re}_{gen} \tag{5}$$

where

$$\mathrm{Re}_{gen} = \frac{\rho D^n U^{2-n}}{8^{n-1} k \left(\frac{3n+1}{4n}\right)^n} \tag{6}$$

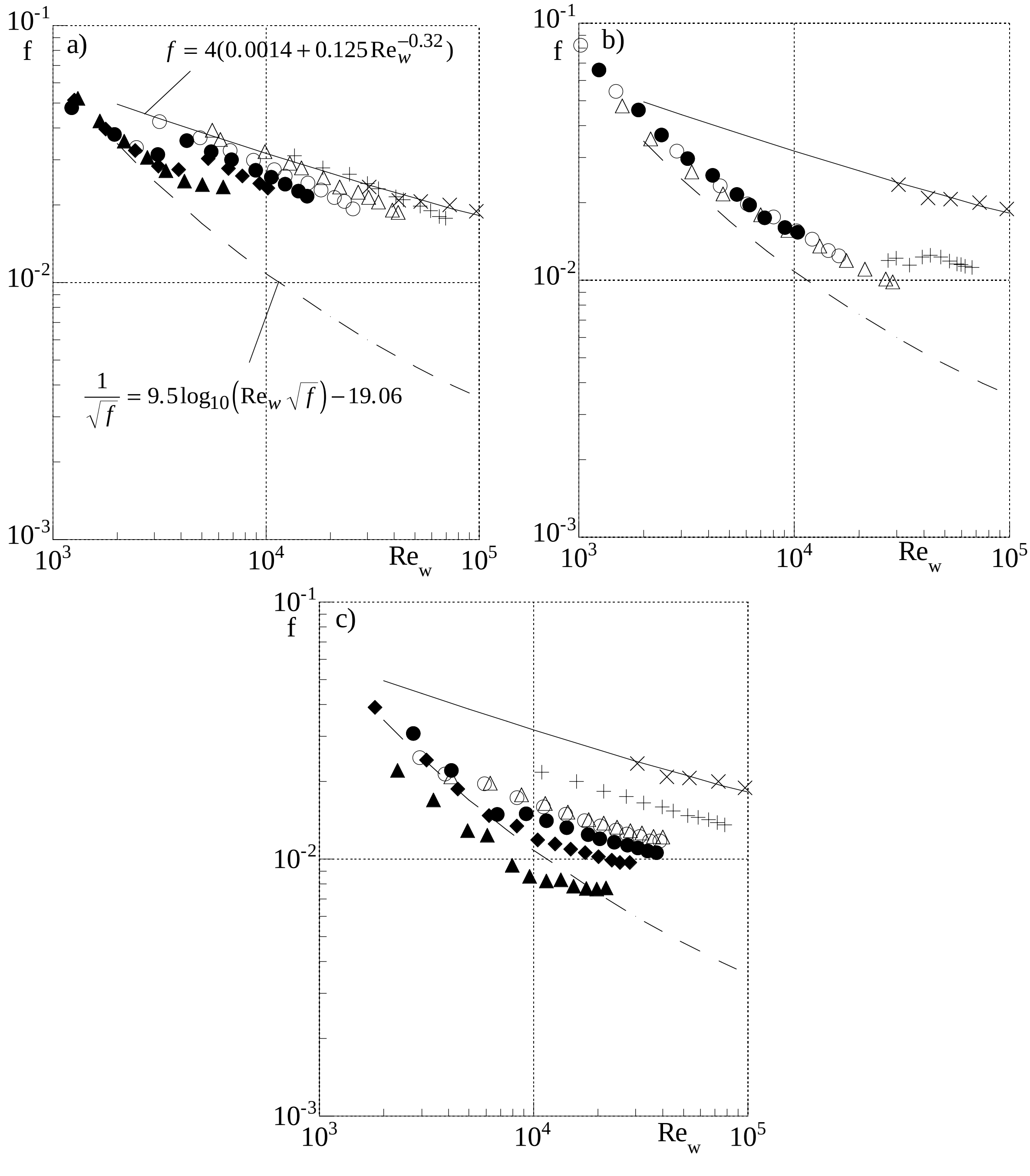

Figure 4) Variation of the friction factor with the wall Reynolds number. a) Tylose solutions: x water; + 0.1%; Δ 0.2%; O 0.3%; J 0.4% ; F 0.5%; H 0.6%. b) CMC solutions: x water; + 0.1%; Δ 0.2%; O 0.3%; J 0.4%. c) Xanthan gum solutions: x water; + 0.05%; Δ 0.1%; O 0.125%; J 0.15%; F 0.2%; H 0.25%.

In Eq. (6) k and n represent the consistency and power law indices of a power law viscosity model fitted to the measured viscosity at the shear rate range prevailing in each particular pipe flow case having bulk velocity U.

Fig. 3 suggests the possibility of a delay in transition well illustrated by the tylose solutions plots. For all solutions f deviates slowly from the theoretical laminar curve for generalised Reynolds numbers above 2,000. For the 0.4% and 0.5% tylose solutions there is a sudden increase in f at increasing critical Reynolds numbers (at around 2,500 and 3,000, respectively). For the CMC and XG solutions the deviations from the laminar law are also smooth. This is typical of solutions having conditions for the onset of DR in the laminar or early transitional flow regimes, as previously observed by Pinho and Whitelaw (1990) with CMC. As for a true delay of transition a definite determination of the corresponding critical Reynolds number requires a time trace of a quantity, such as the velocity, since a smooth variation in the $f - \mathrm{Re}$ curve can occur in parallel with a sudden increase in the magnitude of velocity fluctuations (Escudier et al, 1992).

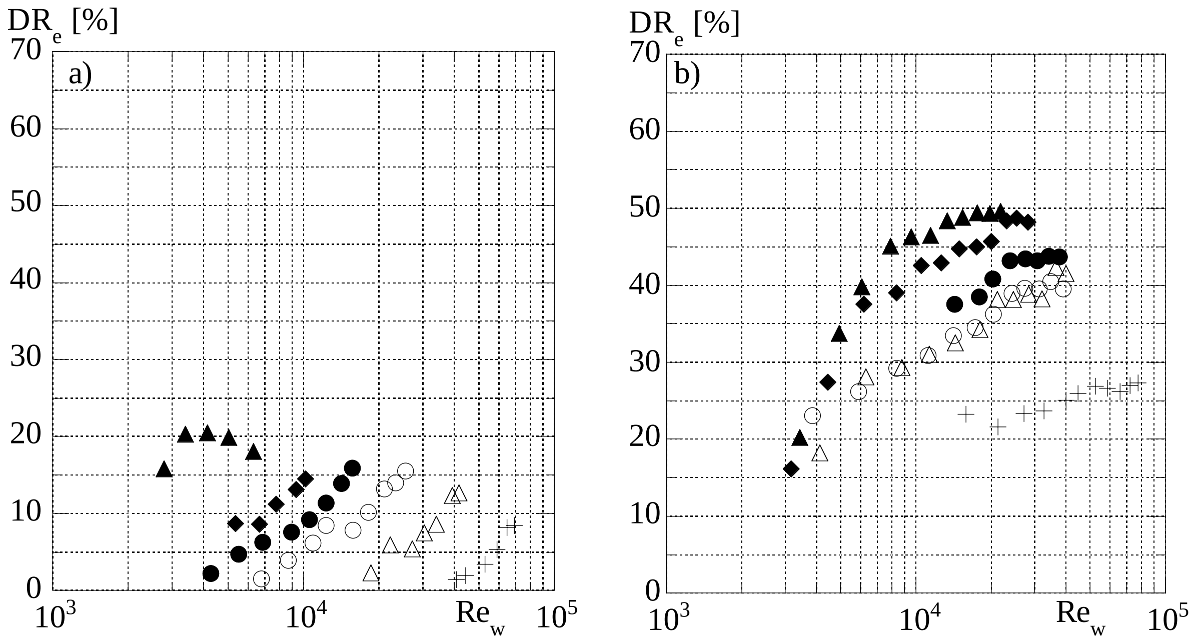

Figure 5) Variation of DR_e with the wall Reynolds number. a) Tylose solutions: + 0.1%; Δ 0.2%; O 0.3%; J 0.4% ; F 0.5%; H 0.6%. b) Xanthan gum solutions: + 0.05%; Δ 0.1%; O 0.125%; J 0.15%; F 0.2%; H 0.25%.

Figs. 4-a), -b) and -c) compare all the measurements for the tylose, CMC and xantham gum solutions, respectively, and each plot includes water measurements, the Newtonian equation of Geiringer (see Idel'cik, 1960) and the maximum drag reduction asymptote of Virk et al (1970). Tylose solutions have the smallest amount of drag reduction and xantham gum solutions the highest. For the three lowest concentrations of tylose there is agreeement between the measurements at low Reynolds numbers and the Newtonian curve suggesting that the onset of drag reduction, observed at higher Reynolds numbers, is taking place under conditions of turbulent flow starting at a critical wall shear stress of about 14 Pa. The drag reduction considered takes into account a non-zero value of $DR - DR_V$. For the three highest concentrations the same wall stress is reached at lower Reynolds numbers, pertaining to the transitional and laminar flow regimes, has hinted by the observation of Fig. 3.

The plots of friction factor of CMC in Fig. 4-b) suggest again that the onset of DR is taking place at laminar flow conditions or that transition is being delayed. The CMC solutions do not reach the maximum DR predicted by Virk, but there is some saturation at about $DR = 60\%$, whereas the 0.2 and 0.25% xanthan gum solutions reach Virk's curve (cf. Fig. 4-c). For the 0.25% XG solution DR even exceeds that predicted by Virk's asymptote. Actually, the asymptote is really an envelope of experimental data under conditions of maximum DR and not a theoretical limit. The effectiveness of XG as a drag reducer, in comparison with the CMC and tylose, stems from its significantly larger size (higher molecular weight) which imparts a higher degree of flexibility to the molecules, and shear-thinning to their solutions, in spite of their semi-rigid structure.

Finally, in Fig. 5-a) and -b) the "elastic" drag reduction ($DR_e \equiv DR - DR_v$) is plotted as a function of Re_w for the tylose and XG solutions. The two plots show well the two different behaviours: for 0.1% to 0.4% tylose solutions DR_e varies in a linear way, expressing a semi-logarithmic variation with Re_w, and tending to cross the x-axis at values of the Reynolds number above 3,000. The absence of this feature for the other solutions confirms that the critical stress for onset of DR is attained in laminar flow. For the XG solutions the maximum value of DR_e is 50%, which corresponds to a total DR= 70% at a Reynolds number of 20,000. So, the viscous drag reduction is significant and accounts to about 30% of the total. Not shown in the graphs is the fact that the solutions of 0.3% and 0.4% CMC have maximum values of DR_e similar to those of 0.2% and 0.25% XG but 30% less DR_v, ie, the differences in the total drag reduction are accounted for by a different shear-thinning intensity and not by a different elastic effect However, note the different additive concentrations required to attain such conditions.

5. CONCLUSIONS

A detailed investigation of the drag reduction behaviour of various non-Newtonian fluids based on tylose, CMC and xanthan gum polymer additives, was carried out in turbulent pipe flow. The results are consistent with previous observations with similar variable viscosity polymer solutions and show that shear-thinning effects can be responsible for a significant proportion of drag reduction. The low molecular weight tylose solutions exhibit small amounts of DR and at the lower concentrations its onset is clearly under conditions of turbulent flow. However, for all CMC and XG solutions and 0.4% and 0.5% tylose solutions the critical wall shear stress for onset of DR is reached in the laminar or early transitional regimes. Although the XG solutions showed higher magnitudes of DR than the CMC, even larger than predicted by Virk's asymptote, a significant proportion was due to the shear-thinning effect which accounted for 30% of the total in some cases, thus resulting in maximum elastic drag reductions similar to those of the CMC solutions, in spite of the larger molecules of the former.

It is expected that in other turbulent flows, such as wall-free flows, the XG solutions will exhibit stronger deviations from the Newtonian fluids than the tylose and CMC solutions both in terms of mean flow as well as in terms of turbulent characteristics.

Acknowledgements

The authors acknowledge the financial support of JNICT through contract number PBICT/CEG/2427/95.

REFERENCES

Coelho, P. M., Pereira, A. S. and Pinho, F. T. 1996. Rheology of tylose, CMC and xanthan gum aqueous solutions. Internal report, Dep. Mech. Eng., University of Porto, Portugal, September.

Coelho, P. M. and Pinho, F. T. 1998. Comportamento Reológico de Algumas Soluções Aquosas Diluídas de Polímero. *Mecânica Experimental*., 3, pp. 51-60.

Den Toonder, J. M. J., Nieuwstadt, F. T. M. and Kuiken, G. D. C. 1995. The role of elongational viscosity in the mechanism of drag reduction by polymer additives. *Applied Sci. Res.*, 54, pp. 95-123.

Dodge, D. W. and Metzner, A. B. 1959. Turbulent flow of non-Newtonian systems. *AIChEJ*, 5, pp. 189-204.

Escudier, M. P., Gouldson, I. W. and Jones, D. M. 1992. Fully developed pipe flow of shear-thinning liquids. Proceedings of the Sixth International Symposium on Applications of Laser Techniques to Fluid Mechanics, Eds. R. Adrian, D. Durão, M. Heitor, M. Maeda, J. Whitelaw, paper 4.6, Lisbon, Portugal.

Escudier, M. P., Gouldson, I. W. and Jones, D. M. 1995. Flow of shear-thinning fluids in concentric annulus. *Exp. in Fluids*, 18, pp. 225-238.

Escudier, M. P., Presti, F. and Smith, S. 1999. Drag reduction in turbulent pipe flow. *J. Non-Newt. Fluid Mech.*, in press.

Hartnett, J. P. 1992. Viscoelastic fluids: a new challenge in heat transfer. *J. Heat Transfer*, 114, pp. 296-303.

Hinch, E. J. 1977. Mechanical models of dilute polymer solutions in strong flows. *Physics of Fluids*, S20, pp. S22-S30.

Hoyt, J. W. 1972. The effect of additives on fluid friction. *Journal of Basic Engineering*, 92, pp. 258-285.

Idel'cik, I. E. 1960. Memento des pertes de charge. Editions Eyrolles, Paris.

Kostic, M. 1994. On turbulent drag and heat transfer reduction phenomena and laminar heat transfer enhancement in non-circular duct flow of certain non-newtonian fluids. *Int. J. Heat and Mass Transfer*, 37, pp. 133-147.

Lumley, J. L., 1977. Drag reduction in two-phase and polymer flows. *Phys. of Fluids*, 20, S64-S71.

Massah, H. and Hanratty, T. J. 1996. The implications of computer studies of the behavior of a FENE bead-spring in a turbulent field. in "FED-Vol. 237, 1996 Fluids Engineering Division Conference, Volume 2, ASME 1996, Drag reduction Conference, San Diego, July 1996, pp. 183-190

Massah, H., Kontomaris, K., Schowalter, W. R. and Hanratty, T. J. 1993. The configurations of a FENE bead-spring chain in transient rheological flows and in a turbulent flow. *Physics of Fluids A*, 5, pp. 881-890.

Metzner, A. B. and Reed, J. C. 1955. Flow of Non-newtonian fluids- correlation of the laminar, transition and turbulent flow regions. *AIChEJ*, 1, pp. 434-440

Myska, J. 1998. Anisotropy of viscosity o drag reducing solution. *AIChEJ*, 44, pp. 1467-1468.

Orlandi, P. 1995. A tentative approach to the direct simulation of drag reduction by polymers. *J. Non-Newt. Fluid Mech.*, 60, pp. 277-301

O'Shaughnessy, B., Durning, C. and Tabor, M. 1990. Polymer deformation in strong high-frequency flows. *Journal Chem. Phys.*, 92, pp. 2637-2645.

Pereira, A. S. and Pinho, F. T. 1994. Turbulent Pipe Flow Characteristics of Low Molecular Weight Polymer Solutions.*J. Non-Newt. Fluid Mech.* 55, pp. 321-344.

Pinho, F. T. and Whitelaw, J. H. 1990. Flow of non-Newtonian fluids in a pipe, *J. Non-Newt. Fluid Mech.*, 34, pp. 129-144.

Virk, P. S., Mickley, H. S. and Smith, Smith, K. A. 1970. The ultimate asymptote and mean flow structure in Toms Phenomena, *Journal of Applied Mechanics*, 92, pp. 488-493.

Virk, P. S. 1975. Drag reduction fundamentals. *AIChEJ*, 21, pp. 625-656.

Zakin, J. L., Myska, J. and Chara, Z. 1996. New limiting drag reduction and velocity profile asymptotes for nonpolymeric additives systems. *AIChEJ*, 42, pp 3544-3546.